IDO is activated in infectious, autoimmune, and malignant diseases that involve cellular immune activation in various organs, including the liver [13]. In fact, upregulation of the IDO expression in the liver and increased serum IDO activity have been found in chronic hepatitis C patients [14,15]. The IDO expression is also enhanced in the liver and adipose tissue in obese individuals [16].

Several rodent studies have revealed the role of IDO in liver injury. In hepatitis B virus (HBV) transgenic mice, the IDO expression in hepatocytes is enhanced in mice with liver injury caused by HBV-specific cytotoxic T lymphocytes [17]. Inhibition of IDO activity exacerbates liver injury in both α-galactosylceramide- and carbon tetrachloride (CCl_4)-induced acute hepatitis models and is associated with the induction of TNF-α [18,19]. These reports suggest that IDO plays a critical role in the regulation of liver inflammation and that targeting IDO activity might be an effective strategy for attenuating acute liver injury. However, the role of IDO in steatosis-induced liver injury has not yet been clarified. In the present study, we examined the effects of IDO on high-fat diet (HFD)-induced liver steatosis and subsequent hepatic inflammation and fibrosis using IDO-deficient mice.

Materials and Methods

2.1 Animals and experimental procedure

This study was carried out in strict accordance with the recommendations of the Guide for the Care and Use of Laboratory Animals of Gifu University Life Science Research Center. The protocol was approved by the Committee on the Ethics of Animal Experiments of Gifu University (Permit Number: 24-65). All surgeries were performed under sodium pentobarbital anesthesia, and all efforts were made to minimize animal suffering. Five-week-old male IDO-wild-type (WT) mice and IDO-knockout (KO) mice with a C57BL/6J background were obtained from The Jackson Laboratory (Bar Harbor, ME, USA). HFD-60 (506.2 kcal/100 g) with 62.2% of the calories derived from fat was purchased from Oriental Yeast (Tokyo, Japan). The cholesterol content of the diet was 33.0 mg/100 g. After 1 week of acclimatization, 8 WT mice and 8 KO mice were given a pelleted HFD throughout the experiment (26 weeks) with free access to tap water and food. At the end of the experiment (32 weeks of age), all mice were sacrificed under sodium pentobarbital anesthesia and the livers were carefully removed.

2.2 Histopathological and immunohistochemical examinations

For all the experimental mice, 4 μm-thick sections of formalin-fixed and paraffin-embedded livers were stained with hematoxylin & eosin (H&E) for conventional histopathology or with Sirius Red stain to determine the presence of liver fibrosis. The histological features of the livers were evaluated using the NAFLD activity score (NAS) system [20]. The computer-assisted quantitative analyses of hepatic fibrosis development were carried out using the BZ-Analyzer-II software program (KEYENCE, Osaka, Japan) [21,22].

In order to evaluate the infiltration of inflammatory cells in the liver, immunohistochemical staining for Mac-1 (a macrophage marker), CD3 (a T-cell marker), and NIMP-R14 (a neutrophil marker) of paraffin-embedded sections was performed using the linked streptavidin-biotin method. Rat monoclonal anti-Mac-1 antibody (MAB1387Z, 1:50 dilution) was purchased from Chemicon International (Temecula, CA, USA). Rabbit polyclonal anti-CD3 (ab5690, 1:100 dilution) antibodies and rat monoclonal anti-neutrophil antibody (NIMP-R14, ab2557, 1:50 dilution) were obtained from Abcam (Cambridge, MA, USA). On the Mac-1-, CD3-, and NIMP-R14-immunostained sections, the inflammatory cells that intensively reacted to these antibodies were counted and the data are expressed as the percentage of total inflammatory cells in the liver. A positive cell index (%) was determined by counting at least 500 cells in a section from each mouse.

2.3 Hepatic hydroxyproline analysis

The hepatic hydroxyproline content (μmol/g wet liver) was quantified colorimetrically in duplicate samples from approximately 200mg of the wet-weight liver tissues, as described previously [22].

2.4 RNA extraction and quantitative real-time RT-PCR analysis

Total RNA was isolated from the livers and adipose tissue of the mice using the RNeasy Mini Kit and RNeasy Lipid Tissue Mini Kit (Qiagen, Hilden, Germany), respectively [21]. cDNA was amplified from 0.5 μg of total RNA using the SuperScript III First-Strand Synthesis System (Invitrogen, Carlsbad, CA, USA). A quantitative real-time reverse transcription-PCR (RT-PCR) analysis was performed using specific primers that amplify F4/80, IFNγ, interleukin (IL)-1β, IL-6, TNF-α, superoxide dismutase (SOD)-1, SOD-2, glutathione peroxidase (GPx), transforming growth factor (TGF)-β1, glyceraldehyde-3-phosphate dehydrogenase (GAPDH), and the ribosomal protein large P0 (RPLP0) genes. The sequences of the primers for these genes, which were obtained from Universal ProbeLibrary Assay Design Center (Roche, Indianapolis, IN, USA), are shown in Table 1. The analysis to quantify the expression levels of tryptophan 2,3-dioxygenase (TDO) was performed using TaqMan Gene Expression Assays (Applied Biosystems, Foster City, CA, USA) and TOYOBO Real-time PCR Master Mix (TOYOBO, Osaka, Japan), as described previously [23]. Each sample was analyzed on a LightCycler Nano (Roche) with FastStart Essential DNA Green Master (Roche). The parallel amplification of GAPDH and RPLP0 was used as the internal control for liver and adipose tissue, respectively.

2.5 Clinical chemistry

The serum levels of alanine aminotransferase (ALT) were measured using a standard clinical automatic analyzer (type 7180; Hitachi, Tokyo, Japan).

Table 1. Primer sequences.

Gene	Primer sequence	
SOD1	F	5'- CAGGACCTCATTTTAATCCTCAC-3'
	R	5'- TGCCCAGGTCTCCAACAT-3'
SOD2	F	5'- TGCTCTAATCAGGACCCATTG-3'
	R	5'- GTAGTAAGCGTGCTCCCACAC-3'
GPx	F	5'- TTTCCCGTGCAATCAGTTC-3'
	R	5'- TCGGACGTACTTGAGGGAAT-3'
F4/80	F	5'- ACAAGACTGACAACCAGACGG-3'
	R	5'- TAGCATCCAGAAGAAGCAGGCGA-3'
IFNγ	F	5'- AGCAACAGCAAGGCGAAAAAG-3'
	R	5'- CGCTTCCTGAGGCTGGATTC-3'
IL-1β	F	5'- CAAGCAACGACAAAATACCTGTG-3'
	R	5'- AGACAAACCGTTTTTCCATCTTCT-3'
IL-6	F	5'- CCGGAGAGGAGACTTCACAGAG-3'
	R	5'- CTGCAAGTGCATCATCGTTGTT-3'
TNF-α	F	5'- TGGCCCAGACCCTCACACTCAG-3'
	R	5'- ACCCATCGGCTGGCACCACT-3'
TGF-β1	F	5'- ACCGGAGAGCCCTGGATACCA-3'
	R	5'- TATAGGGGCAGGGTCCCAGACA-3'
RPLP0	F	5'- ACTGGTCTAGGACCCGAGAAG-3'
	R	5'- CTCCCACCTTGTCTCCAGTC-3'
GAPDH	F	5'-GACATCAAGAAGGTGGTGAAGCAG-3'
	R	5'-ATACCAGGAAATGAGCTTGACAAA-3'

doi: 10.1371/journal.pone.0073404.t001

2.6 Oxidative stress analysis

The serum hydroperoxide levels, one of the markers of oxidative stress, were determined using the derivatives of reactive oxygen metabolites (d-ROM) test (FREE Carpe Diem; Diacron s.r.l., Grosseto, Italy), according to the manufacturer's protocol.

2.7 Determination of the enzymatic activity of IDO

The IDO activity level in the serum was determined by calculating the ratio of the L-kynurenine/L-tryptophan concentrations [23]. Serum samples were deproteinized with 3% perchloric acid. Following centrifugation, aliquots of supernatant were collected to determine the concentrations of L-tryptophan and L-kynurenine using HPLC, as described previously [18].

2.8 Hepatic lipid analysis

After total lipids were extracted from the frozen livers (approximately 200 mg), the triglyceride levels were measured using the triglyceride E-test kit (Wako, Osaka, Japan) [21].

2.9 Statistical analysis

The data are expressed as the mean ± SD. Statistical significance of the difference between mean values was evaluated using the Mann-Whitney *U* test. Significance was defined as a *P* value less than 0.05.

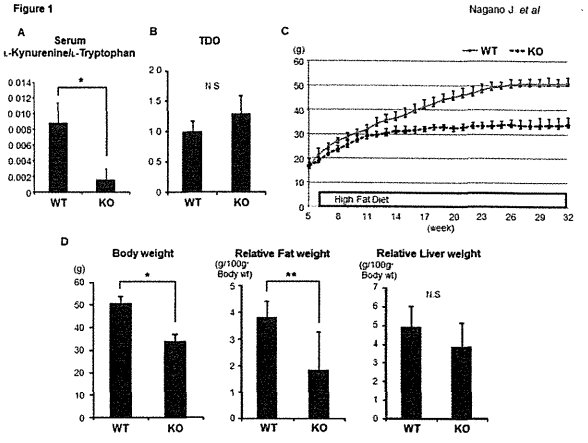

Figure 1. Effects of IDO deficiency on the serum L-kynurenine/L-tryptophan ratio, the expression levels of TDO in the liver, the growth curve, and the body, liver, and fat weights of the experimental mice. (A) The functional IDO activity level was determined by measuring the concentrations of L-kynurenine and L-tryptophan using HPLC. The L-kynurenine/L-tryptophan ratio indicates the IDO activity. (B) Total RNA was isolated from the livers of the experimental mice, and the expression levels of TDO mRNA were examined using quantitative real-time RT-PCR with specific primers. (C) The growth curve of the experimental mice. The body weights of all mice were measured once a week during the experiment. (D) The body weights and relative weights of the adipose tissues and livers of the experimental mice at the termination of the study. The values are expressed as the mean ± SD. * $P < 0.001$, ** $P < 0.05$.

doi: 10.1371/journal.pone.0073404.g001

Results

3.1 General observations

We initially examined the enzymatic activity of IDO in the serum of the experimental mice by measuring the concentrations of L-kynurenine and L-tryptophan. The L-kynurenine/L-tryptophan ratios in serum of the IDO-KO mice were significantly lower than those in the serum of the IDO-WT mice (Figure 1A, $P < 0.001$), indicating that IDO activity was clearly inhibited in the IDO-KO mice. TDO, a hepatic enzyme that catalyses the first step of tryptophan degradation, was expressed in the liver in both the IDO-WT mice and the IDO-KO mice; however, IDO deficiency did not have a significant effect on the TDO mRNA expression (Figure 1B). Figure 1C shows the growth curves of the mice during this experiment. The body weight gain of the IDO-KO mice was smaller than that of the IDO-WT mice. At the end of the experiment, the body weights (Figure 1D, $P < 0.001$) and the relative weights of the adipose tissues of the IDO-KO mice (Figure 1D, $P < 0.05$) were also significantly lower than those of the IDO-WT mice.

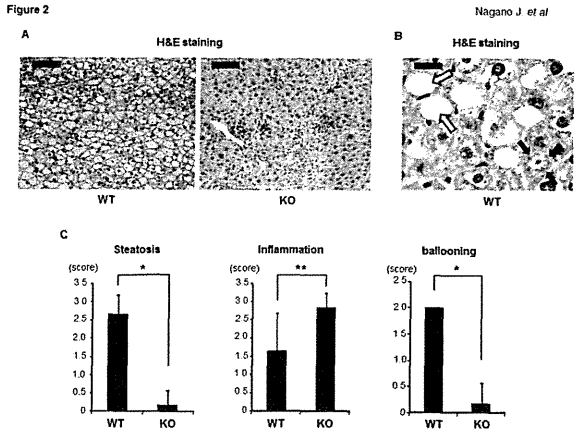

Figure 2. Effects of IDO deficiency on hepatic histopathology in the experimental mice. (A) and (B) H&E staining of liver sections from the experimental mice. (A) Representative photomicrographs of the liver sections of the IDO-WT mice and IDO-KO mice (low-power field). Black bar: 100 μm. (B) An enlarged photo (high-power field) of the liver sections from the IDO-WT mice. Ballooned hepatocytes (indicated by white arrows) and Mallory-Denk bodies (indicated by black arrows) were observed. Black bar: 20 μm. (C) The presence of NAS (steatosis, inflammation, and ballooning) was determined based on the histopathological analysis. The values are expressed as the mean ± SD. * P <0.001, ** P <0.05.

doi: 10.1371/journal.pone.0073404.g002

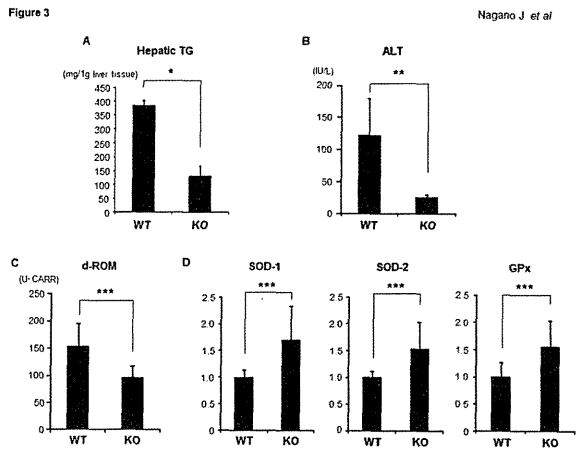

Figure 3. Effects of IDO deficiency on intrahepatic triglycerides, the serum ALT levels, and oxidative stress in the experimental mice. (A) Hepatic lipids were extracted from the frozen livers of the experimental mice, and the triglyceride levels were measured. (B) At sacrifice, blood samples were collected and the serum levels of ALT were assayed. (C) The hydroperoxide levels in the serum at the end of the experiment were determined using the d-ROM test. (D) Total RNA was isolated from the livers of the experimental mice, and the expression levels of SOD-1, SOD-2, and GPx mRNA were examined using quantitative real-time RT-PCR with specific primers. The values are expressed as the mean ± SD. * P <0.001, ** P <0.01, *** P <0.05.

doi: 10.1371/journal.pone.0073404.g003

3.2 Effects of IDO deficiency on hepatic histopathology in the experimental mice

The H&E staining results of the livers of the IDO-KO mice and IDO-WT mice after 26 weeks of being fed the HFD are presented in Figure 2A and B. The infiltration of inflammatory cells was markedly increased in the livers of the IDO-KO mice, and the NAS inflammation scores were significantly higher than those in the IDO-WT mice (Figure 2C, $P < 0.05$). Interestingly, the hepatic steatosis and ballooning degeneration of hepatocytes were lower in the IDO-KO mice than in the IDO-WT mice at this experimental time point (Figure 2C, $P < 0.001$). In addition to the ballooned hepatocytes, Mallory-Denk bodies, which are a recognized feature of alcoholic hepatitis and NASH [24], were also observed in the liver of IDO-WT mice (Figure 2B).

3.3 Effects of IDO deficiency on the intrahepatic triglyceride levels, the serum ALT levels, and oxidative stress in the experimental mice

The histological findings were consistent with the measured intrahepatic triglyceride contents: the levels of triglycerides in the livers of the IDO-KO mice were significantly lower than those in the livers of the IDO-WT mice (Figure 3A, $P < 0.001$). The serum levels of ALT in the IDO-KO mice were also significantly decreased relative to those in the IDO-WT mice (Figure 3B, $P < 0.01$). In addition, the serum d-ROM levels, which reflect the serum hydroperoxide levels, were significantly lower in the IDO-KO mice than in the IDO-WT mice (Figure 3C, $P < 0.05$). Compared to the IDO-WT mice, there were also significant increases in the expression levels of SOD-1, SOD-2, and GPx mRNA, which encode antioxidant enzymes, in the livers of the IDO-KO mice (Figure 3D, $P < 0.05$). These findings indicate that hepatic triglyceride accumulation and oxidative stress are reduced, while antioxidant activity is increased, in mice lacking the IDO gene.

3.4 Effects of IDO deficiency on inflammation in the livers and WAT of the experimental mice

We next examined the expression levels of inflammatory mediators that are implicated in the progression of fatty liver to NASH [7] in the experimental mice. A quantitative real-time RT-PCR analysis revealed that the expression levels of F4/80, a marker of macrophages, were significantly increased in the livers of the IDO-KO mice in comparison to those observed in the livers of the IDO-WT mice (Figure 4A, $P < 0.01$). There were also significant increases in the expression levels of inflammatory mediators, including IFNγ, IL-1β, and IL-6 mRNA, in the livers of the IDO-KO mice compared to those observed in the livers of the IDO-WT mice (Figure 4A, $P < 0.05$). The expression levels of TNF-α mRNA were also higher in the livers of the IDO-KO mice than in the livers of the IDO-WT mice;

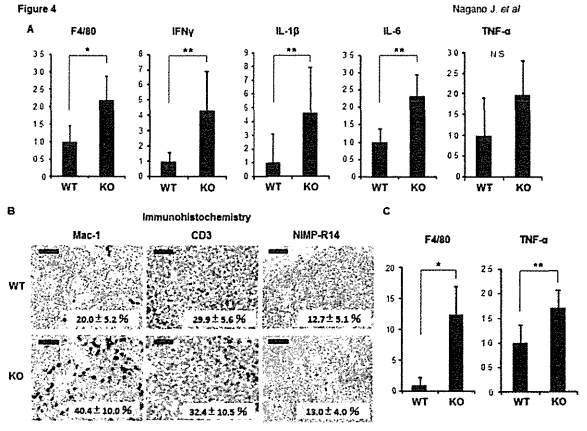

Figure 4. Effects of IDO deficiency on the inflammation in the liver and white adipose tissue of the experimental mice. (A) The expression levels of F4/80, IFNγ, IL-1β, IL-6, and TNF-α mRNA in the livers of the experimental mice. (B) The results of the immunohistochemical analyses of Mac-1, CD3, and NIMP-R14 in the livers of the experimental mice. A positive cell index (%) was shown in each photo. Black bar: 50 μm. (C) The expression levels of F4/80 and TNF-α mRNA in the WAT of the experimental mice. Total RNA was isolated from the livers (A) and WAT (C) of the experimental mice, and the expression levels of each mRNA were examined using quantitative real-time RT-PCR with specific primers. The expression levels of GAPDH mRNA and RPLP0 mRNA were used as internal controls for the liver and WAT, respectively. The values are expressed as the mean ± SD. * P <0.01, ** P <0.05.

doi: 10.1371/journal.pone.0073404.g004

however, the difference was insignificant (Figure 4A). Furthermore, the immunohistochemical analyses demonstrated that the inflammatory cells that had infiltrated into the livers of the IDO-KO mice positively reacted with either the anti-Mac-1(40.4 ± 10.0%) or anti-CD3 (32.4 ± 10.5%) antibodies. On the other hand, the infiltration of neutrophils (13.0 ± 4.0%) was low compared to that of macrophages and T-cells. These findings suggest that macrophages and T lymphocytes were the predominantly increased cell populations in the livers of the IDO-KO mice. The infiltration of Mac-1 positive cells in the livers of IDO-KO mice (40.4 ± 10.0%) was high compared to that of IDO-WT mice (20.0 ± 5.2%) (Figure 4B, $P < 0.05$), and this is consistent with the results of RT-PCR analysis showing the increased levels of F4/80 mRNA in the livers of IDO-KO mice (Figure 4A).

Moreover, as shown in Figure 4C, the expression levels of F4/80 ($P < 0.01$) and TNF-α($P < 0.05$) mRNA in WAT were both significantly increased in the IDO-KO mice compared to those observed in the IDO-WT mice, indicating that inflammation is augmented in WAT, in addition to the liver, in the IDO-KO mice [24].

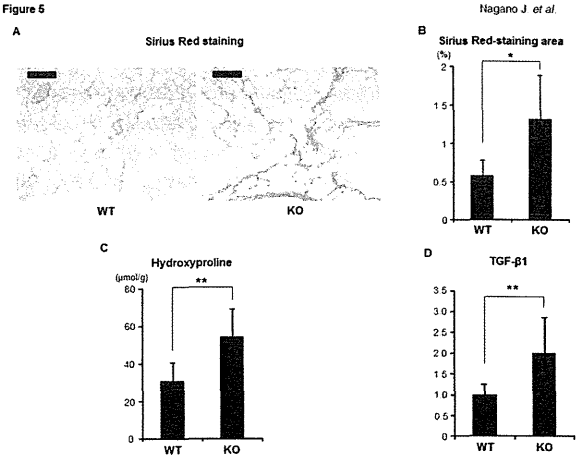

Figure 5. Effects of IDO deficiency on the hepatic fibrosis in the experimental mice. (A) Representative photomicrographs of liver sections stained with Sirius Red to show fibrosis. Black bar: 100 μm. (B) The Sirius Red-stained images of fibrosis were analyzed using a BZ-9000 fluorescence microscope, and the fibrotic area was measured using a BZ-Analyzer-II. (C) The hepatic hydroxyproline contents were quantified colorimetrically. (D) Total RNA was isolated from the livers of the experimental mice, and the expression levels of TGF-β1 mRNA were examined using quantitative real-time RT-PCR with specific primers. The values are expressed as the mean ± SD. * P <0.01, ** P <0.05.

doi: 10.1371/journal.pone.0073404.g005

3.5 Effects of IDO deficiency on hepatic fibrosis in the experimental mice

We next examined whether IDO deficiency has an effect on the development of steatosis-induced hepatic fibrosis. An examination of Sirius Red-stained sections indicated that, compared to the IDO-WT mice, the IDO-KO mice markedly developed pericellular fibrosis in the liver (Figure 5A and B, $P < 0.01$). Similar findings were observed in the measured hepatic hydroxyproline contents: the IDO-KO mice showed a significant increase in the amount of hydroxyproline observed in the liver (Figure 5C, $P < 0.05$). The expression levels of TGF-β1 mRNA, a central regulator of chronic liver disease contributing to fibrogenesis through inflammation [25], were also remarkably elevated in the livers of the IDO-KO mice compared to those observed in the livers of the IDO-WT mice (Figure 5D, $P < 0.05$). These findings may indicate that IDO-KO mice are susceptible to the development of steatosis-induced hepatic fibrosis.

Discussion

The results of the present study indicate that HFD-induced hepatic inflammation and fibrosis are significantly aggravated in IDO-KO mice, although the level of hepatic steatosis and amount of oxidative stress were lower compared to those in IDO-WT mice. Therefore, IDO deficiency is critically involved in

the acceleration of hepatic inflammation observed in the present study.

IDO is a rate-limiting enzyme that can degrade tryptophan via the kynurenine pathway. Because the IDO expression and its enzymatic activity, which are tightly controlled by several immune mediators such as IFNγ, play a key role in the suppression of the immune response [8–11], inhibiting the expression and activity of IDO might promote inflammatory signaling. Therefore, based on our present results, we consider that IDO-deficient mice are more susceptible to the induction of inflammation by HFD. Our results are consistent with those of recent reports showing that the inhibition of the enzymatic activity of IDO significantly exacerbated liver injury in α-galactosylceramide (α-GalCer)- and CCl_4-induced acute hepatitis animal models via the upregulation of IL-6 and TNF-α [18,19]. When the IDO-KO mice were treated with α-GalCer, the production of TNF-α from the infiltrating macrophages in the liver was significantly accelerated, and thus led to the development of severe hepatitis [18]. Therefore, in the present study, the increase in the number of hepatic macrophages might have been critically involved in the exacerbation of HFD-induced hepatic inflammation in the IDO-KO mice. These reports [18,19], together with the results of the present study, suggest that IDO may play a critical role in suppressing excess induction and progression of inflammation in the liver.

Innate immune cells, including Kupffer cells, natural killer T cells, and natural killer cells, play important roles in the excessive production of hepatic T helper 1 cytokines, which is associated with the development of steatohepatitis [4]. The regulation of the immune response by IDO is predominantly based on the ability of IDO to suppress the activation of lymphocytes [9–11]. An increased IDO activity inhibits proliferation and induces apoptosis in T cells and natural killer cells via tryptophan depletion and the production of toxic tryptophan metabolites [9]. In addition, recent studies have revealed that IDO inhibits T cell activation by driving the development of Tregs [10,11]. Tregs, which are actively engaged in the negative control of a variety of immune responses, are recognized as being one of the key players in hepatic immune regulation [26]. HFD-induced steatosis in mice is associated with the depletion of hepatic Tregs and leads to upregulation of the inflammatory pathway [27]. Therefore, an IDO deficiency may increase T cell activation, either directly or indirectly, by suppressing Tregs and thus contributed to a worsening of hepatic inflammation in the present study.

Obesity is associated with systemic low-grade inflammation and immune activation [5,6]. One clinical trial reported that activation of IDO is associated with reduced plasma tryptophan levels in obese patients [28]. IDO is also overexpressed in the liver and adipose tissue in obese subjects [16]. These reports indicate that the overexpression and activation of IDO are implicated in chronic immune activation in obese individuals. T cell infiltration into WAT and subsequent recruitment and activation of macrophages can induce TNF-α production, which is associated with the development of systemic inflammation [5,6]. The present study showed that the expression levels of F4/80 and TNF-α mRNA in WAT are elevated in IDO-KO mice compared to those observed in IDO-WT mice when the mice are fed an HFD, indicating that inflammation of WAT induced by HFD is worsened in IDO deficiency mice. Therefore, our findings suggest that IDO might have the ability to attenuate overactive immune responses caused by obesity in WAT in addition to the liver.

There are some possible limitations associated with the present study. For instance, a recent study demonstrated that neither the overexpression of IDO nor inhibition of its enzymatic activity affected the lipid accumulation in the liver, although the combination of L-tryptophan treatment and a high fat and high fructose diet exacerbated the hepatic steatosis [29]. Therefore, further experiments will be required to clarify the role of IDO and the L-kynurenine/L-tryptophan pathway in the development of hepatic steatosis. Furthermore, after 26 weeks of being fed the HFD, the IDO-KO mice showed lower steatosis and oxidative stress than the IDO-WT mice. The hepatocyte ballooning, which indicates hepatocyte injury, was also decreased in IDO-KO mice compared to IDO-WT mice. These findings seem paradoxical given the enhanced inflammation and fibrosis in IDO-KO mice in response to the HFD. A possible explanation might be that the liver inflammation proceeded earlier in IDO-KO mice, in a similar manner to NAFLD in the clinical setting, where many cases with NAFLD show the disappearance of steatosis during its natural history, while exhibiting severe fibrosis and cirrhosis in the late stages [30,31]. In order to verify this possibility, time course studies that evaluate the levels of hepatic injury, steatosis, and inflammation caused by HFD in the early phase should be conducted. In addition, a recent study revealed that hepatic fat deposits were broken down to provide energy for fibrogenesis in a CCl_4-treated mouse model [32]. Such a mechanism might have also been active in our HFD-fed IDO-KO mice, but again, further experiments will be required to confirm this hypothesis.

In conclusion, we herein demonstrated that IDO deficiency worsens hepatic and WAT inflammation in mice fed an HFD. Our findings suggest that regulation of the IDO-mediated immune response might be an interesting strategy for managing steatosis-related hepatic injury.

Author Contributions

Performed the experiments: JN YS TK NN HO. Analyzed the data: JN MS TT. Wrote the manuscript: JN MS TH HI TT HT KS MS HM.

References

1. Angulo P (2002) Nonalcoholic fatty liver disease. N Engl J Med 346: 1221-1231. doi:10.1056/NEJMra011775. PubMed: 11961152.
2. Farrell GC, Larter CZ (2006) Nonalcoholic fatty liver disease: from steatosis to cirrhosis. Hepatology 43: S99-S112. doi:10.1002/hep.20973. PubMed: 16447287.
3. Cusi K (2012) Role of obesity and lipotoxicity in the development of nonalcoholic steatohepatitis: pathophysiology and clinical implications. Gastroenterology 142: 711-725 e716 doi:10.1053/j.gastro.2012.02.003. PubMed: 22326434.
4. Zhan YT, An W (2010) Roles of liver innate immune cells in nonalcoholic fatty liver disease. World J Gastroenterol 16: 4652-4660. doi:10.3748/wjg.v16.i37.4652. PubMed: 20872965.
5. Chatzigeorgiou A, Karalis KP, Bornstein SR, Chavakis T (2012) Lymphocytes in obesity-related adipose tissue inflammation. Diabetologia 55: 2583-2592. doi:10.1007/s00125-012-2607-0. PubMed: 22733483.
6. Weisberg SP, McCann D, Desai M, Rosenbaum M, Leibel RL et al. (2003) Obesity is associated with macrophage accumulation in adipose tissue. J Clin Invest 112: 1796-1808. doi:10.1172/JCI19246. PubMed: 14679176.
7. Fujii H, Kawada N (2012) Inflammation and fibrogenesis in steatohepatitis. J Gastroenterol 47: 215-225. doi:10.1007/s00535-012-0527-x. PubMed: 22310735.
8. Fallarino F, Grohmann U, Puccetti P (2012) Indoleamine 2,3-dioxygenase: from catalyst to signaling function. Eur J Immunol 42: 1932-1937. doi:10.1002/eji.201242572. PubMed: 22865044.
9. Frumento G, Rotondo R, Tonetti M, Damonte G, Benatti U et al. (2002) Tryptophan-derived catabolites are responsible for inhibition of T and natural killer cell proliferation induced by indoleamine 2,3-dioxygenase. J Exp Med 196: 459-468. doi:10.1084/jem.20020121. PubMed: 12186838.
10. Mellor AL, Munn DH (2004) IDO expression by dendritic cells: tolerance and tryptophan catabolism. Nat Rev Immunol 4: 762-774. doi:10.1038/nri1457. PubMed: 15459668.
11. Munn DH (2011) Indoleamine 2,3-dioxygenase, Tregs and cancer. Curr Med Chem 18: 2240-2246. doi:10.2174/092986711795656045. PubMed: 21517755.
12. Dienes HP, Drebber U (2010) Pathology of immune-mediated liver injury. Dig Dis 28: 57-62. doi:10.1159/000282065. PubMed: 20460891.
13. Schröcksnadel K, Wirleitner B, Winkler C, Fuchs D (2006) Monitoring tryptophan metabolism in chronic immune activation. Clin Chim Acta 364: 82-90. doi:10.1016/j.cca.2005.06.013. PubMed: 16139256.
14. Larrea E, Riezu-Boj JI, Gil-Guerrero L, Casares N, Aldabe R et al. (2007) Upregulation of indoleamine 2,3-dioxygenase in hepatitis C virus infection. J Virol 81: 3662-3666. doi:10.1128/JVI.02248-06. PubMed: 17229698.
15. Higashitani K, Kanto T, Kuroda S, Yoshio S, Matsubara T et al. (2012) Association of enhanced activity of indoleamine 2,3-dioxygenase in dendritic cells with the induction of regulatory T cells in chronic hepatitis C infection. J Gastroenterol, 48: 660–70. PubMed: 22976933.
16. Wolowczuk I, Hennart B, Leloire A, Bessede A, Soichot M et al. (2012) Tryptophan metabolism activation by indoleamine 2,3-dioxygenase in adipose tissue of obese women: an attempt to maintain immune homeostasis and vascular tone. Am J Physiol Regul Integr Comp Physiol 303: R135-R143. doi:10.1152/ajpregu.00373.2011. PubMed: 22592557.
17. Iwamoto N, Ito H, Ando K, Ishikawa T, Hara A et al. (2009) Upregulation of indoleamine 2,3-dioxygenase in hepatocyte during acute hepatitis caused by hepatitis B virus-specific cytotoxic T lymphocytes in vivo. Liver Int 29: 277-283. doi:10.1111/j.1478-3231.2008.01748.x. PubMed: 18397228.
18. Ito H, Hoshi M, Ohtaki H, Taguchi A, Ando K et al. (2010) Ability of IDO to attenuate liver injury in alpha-galactosylceramide-induced hepatitis model. J Immunol 185: 4554-4560. doi:10.4049/jimmunol.0904173. PubMed: 20844202.
19. Li D, Cai H, Hou M, Fu D, Ma Y et al. (2012) Effects of indoleamine 2,3-dioxygenases in carbon tetrachloride-induced hepatitis model of rats. Cell Biochem Funct 30: 309-314. doi:10.1002/cbf.2803. PubMed: 22249930.
20. Kleiner DE, Brunt EM, Van Natta M, Behling C, Contos MJ et al. (2005) Design and validation of a histological scoring system for nonalcoholic fatty liver disease. Hepatology 41: 1313-1321. doi:10.1002/hep.20701. PubMed: 15915461.
21. Terakura D, Shimizu M, Iwasa J, Baba A, Kochi T et al. (2012) Preventive effects of branched-chain amino acid supplementation on the spontaneous development of hepatic preneoplastic lesions in C57BL/KsJ-db/db obese mice. Carcinogenesis, 33: 2499–506. PubMed: 23027617.
22. Yasuda Y, Shimizu M, Sakai H, Iwasa J, Kubota M et al. (2009) (-)-Epigallocatechin gallate prevents carbon tetrachloride-induced rat hepatic fibrosis by inhibiting the expression of the PDGFRbeta and IGF-1R. Chem Biol Interact 182: 159-164. doi:10.1016/j.cbi.2009.07.015. PubMed: 19646978.
23. Ogawa K, Hara T, Shimizu M, Ninomiya S, Nagano J et al. (2012) Suppression of azoxymethane-induced colonic preneoplastic lesions in rats by 1-methyltryptophan, an inhibitor of indoleamine 2,3-dioxygenase. Cancer Sci 103: 951-958. doi:10.1111/j.1349-7006.2012.02237.x. PubMed: 22320717.
24. Machado MV, Cortez-Pinto H (2011) Cell death and nonalcoholic steatohepatitis: where is ballooning relevant? Expert Rev Gastroenterol Hepatol 5: 213-222. doi:10.1586/egh.11.16. PubMed: 21476916.
25. Dooley S, ten Dijke P (2012) TGF-beta in progression of liver disease. Cell Tissue Res 347: 245-256. doi:10.1007/s00441-011-1246-y. PubMed: 22006249.
26. Chang KM (2005) Regulatory T cells and the liver: a new piece of the puzzle. Hepatology 41: 700-702. doi:10.1002/hep.20678. PubMed: 15789365.
27. Ma X, Hua J, Mohamood AR, Hamad AR, Ravi R et al. (2007) A high-fat diet and regulatory T cells influence susceptibility to endotoxin-induced liver injury. Hepatology 46: 1519-1529. doi:10.1002/hep.21823. PubMed: 17661402.
28. Brandacher G, Winkler C, Aigner F, Schwelberger H, Schroecksnadel K et al. (2006) Bariatric surgery cannot prevent tryptophan depletion due to chronic immune activation in morbidly obese patients. Obes Surg 16: 541-548. doi:10.1381/096089206776945066. PubMed: 16687019.
29. Osawa Y, Kanamori H, Seki E, Hoshi M, Ohtaki H et al. (2011) L-tryptophan-mediated enhancement of susceptibility to nonalcoholic fatty liver disease is dependent on the mammalian target of rapamycin. J Biol Chem 286: 34800-34808. doi:10.1074/jbc.M111.235473. PubMed: 21841000.
30. Maheshwari A, Thuluvath PJ (2006) Cryptogenic cirrhosis and NAFLD: are they related? Am J Gastroenterol 101: 664-668. doi:10.1111/j.1572-0241.2006.00478.x. PubMed: 16464222.
31. Caldwell SH, Lee VD, Kleiner DE, Al-Osaimi AM, Argo CK et al. (2009) NASH and cryptogenic cirrhosis: a histological analysis. Ann Hepatol 8: 346-352. PubMed: 20009134.
32. Hernández-Gea V, Ghiassi-Nejad Z, Rozenfeld R, Gordon R, Fiel MI et al. (2012) Autophagy releases lipid that promotes fibrogenesis by activated hepatic stellate cells in mice and in human tissues. Gastroenterology 142: 938-946. doi:10.1053/j.gastro.2011.12.044. PubMed: 22240484.

Baba et al. BMC Cancer 2013, 13:465
http://www.biomedcentral.com/1471-2407/13/465

BMC Cancer

RESEARCH ARTICLE Open Access

Synergistic growth inhibition by acyclic retinoid and phosphatidylinositol 3-kinase inhibitor in human hepatoma cells

Atsushi Baba, Masahito Shimizu*, Tomohiko Ohno, Yohei Shirakami, Masaya Kubota, Takahiro Kochi, Daishi Terakura, Hisashi Tsurumi and Hisataka Moriwaki

Abstract

Background: A malfunction of RXRα due to phosphorylation is associated with liver carcinogenesis, and acyclic retinoid (ACR), which targets RXRα, can prevent the development of hepatocellular carcinoma (HCC). Activation of PI3K/Akt signaling plays a critical role in the proliferation and survival of HCC cells. The present study examined the possible combined effects of ACR and LY294002, a PI3K inhibitor, on the growth of human HCC cells.

Methods: This study examined the effects of the combination of ACR plus LY294002 on the growth of HLF human HCC cells.

Results: ACR and LY294002 preferentially inhibited the growth of HLF cells in comparison with Hc normal hepatocytes. The combination of 1 μM ACR and 5 μM LY294002, in which the concentrations used are less than the IC_{50} values of these agents, synergistically inhibited the growth of HLF, Hep3B, and Huh7 human HCC cells. These agents when administered in combination acted cooperatively to induce apoptosis in HLF cells. The phosphorylation of RXRα, Akt, and ERK proteins in HLF cells were markedly inhibited by treatment with ACR plus LY294002. Moreover, this combination also increased RXRE promoter activity and the cellular levels of RARβ and $p21^{CIP1}$, while decreasing the levels of cyclin D1.

Conclusion: ACR and LY294002 cooperatively increase the expression of RARβ, while inhibiting the phosphorylation of RXRα, and that these effects are associated with the induction of apoptosis and the inhibition of cell growth in human HCC cells. This combination might therefore be effective for the chemoprevention and chemotherapy of HCC.

Keywords: Acyclic retinoid, LY294002, Hepatocellular carcinoma, RXRα, Synergism

Background

Retinoids, vitamin A metabolites and analogs, are ligands of the nuclear receptor superfamily that exert fundamental effects on cellular activities, including growth, differentiation, and death (regulation of apoptosis). Retinoids exert their biological functions primarily by regulating gene expression through 2 distinct nuclear receptors, the retinoic acid receptors (RARs) and retinoid X receptors (RXRs), which are ligand-dependent transcription factors [1,2]. Among retinoid receptors, RXRs are regarded as master regulators of the nuclear receptor superfamily because they play an essential role in controlling normal cell proliferation and metabolism by acting as common heterodimerization partners for various types of nuclear receptors [1,2]. Therefore, altered expression and function of RXRs are strongly associated with the development of various disorders, including cancer, whereas targeting RXRs by retinoids might be an effective strategy for the prevention and treatment of human malignancies [3].

Hepatocellular carcinoma (HCC) is one of the most frequently occurring cancers worldwide. Recent studies have revealed that a malfunction of RXRα, one of the subtypes of RXR, due to aberrant phosphorylation by the Ras/mitogen-activated protein kinase (MAPK) signaling pathway is profoundly associated with liver carcinogenesis [4-9]. On the other hand, a prospective randomized study showed that administration of acyclic retinoid (ACR), a

* Correspondence: shimim-gif@umin.ac.jp
Department of Gastroenterology, Gifu University Graduate School of Medicine, Graduate School of Medicine, 1-1 Yanagido, Gifu 501-1194, Japan

synthetic retinoid which targets RXRα, inhibited the development of a second primary HCC, and thus improved patient survival from this malignancy [10,11]. ACR inhibits the growth of HCC-derived cells via the induction of apoptosis by working as a ligand for retinoid receptors [12,13]. ACR also suppresses HCC cell growth and inhibits the development of liver tumors by inhibiting the activation and expression of several types of growth factors and their corresponding receptor tyrosine kinases (RTKs), which lead to the inhibition of the Ras/MAPK activation and RXRα phosphorylation [8,9,14-17]. These reports strongly suggest that ACR might be a promising agent for the prevention and treatment of HCC.

Phosphatidylinositol 3-kinase (PI3K) is activated by growth factor stimulation through RTKs and Ras activation, and plays a critical role in cell survival and proliferation in collaboration with its major downstream effector Akt, a serine-threonine kinase [18-20]. Increasing evidence has shown that aberrant activation of the PI3K/Akt pathway is implicated in the initiation and progression of several types of human malignancies, including HCC, indicating that targeting PI3K/Akt signaling might be an effective strategy for the treatment of cancers [18-22]. Several clinical trials have been conducted to investigate the safety and anti-cancer effects of therapeutic agents that inhibit the PI3K/Akt signaling cascade [18-20]. Combined treatment with a PI3K/Akt inhibitor and other agents, including MAPK inhibitors, might also be a promising regimen that exerts potent anti-cancer properties [23,24].

Combination therapy and prevention using ACR as a key drug is promising for HCC treatment because ACR can act synergistically with other agents in suppressing growth and inducing apoptosis in human HCC-derived cells [17,25-30]. The aim of the present study is to investigate whether the combination of ACR plus LY294002, a PI3K inhibitor, exerts synergistic growth inhibitory effects on human HCC cells, and to examine possible mechanisms for such synergy, predominantly focusing on the inhibitory effects on RXRα phosphorylation by a combination of these agents.

Methods

Materials

ACR (NIK-333) was supplied by Kowa Pharmaceutical (Tokyo, Japan). LY294002 was purchased from Wako (Osaka, Japan). Another PI3K inhibitor NVP-BKM120 (BKM120) was from Selleck Chemicals (Houston, TX, USA).

Cell lines and cell culture conditions

HLF, Huh7, Hep3B, and HepG2 human HCC cell lines were obtained from the Japanese Cancer Research Resources Bank (Tokyo, Japan) and were maintained in Dulbecco's Modified Eagle Medium (DMEM) supplemented with 10% FCS and 1% penicillin/streptomycin. The Hc human normal hepatocyte cell line was purchased from Cell Systems (Kirkland, WA, USA) and maintained in CS-S complete medium (Cell Systems). These cells were cultured in an incubator with humidified air containing 5% CO_2 at 37°C.

Cell proliferation assays

Three thousand HCC (HLF, Huh7, Hep3B, and HepG2) or Hc cells were seeded on 96-well plates in serum-free medium. Twenty-four hours later, the cells were treated with the indicated concentrations of ACR or LY294002 for 48 hours in DMEM supplemented with 1% FCS. Cell proliferation assays were performed using a MTS assay (Promega, Madison, WI, USA) according to the manufacturer's instructions. The combination index (CI)-isobologram was used to determine whether the combined effects of ACR plus LY294002 were synergistic [25,27,30,31]. HLF cells were also treated with a combination of the indicated concentrations of ACR and BKM120 for 48 hours to examine whether this combination synergistically inhibited the growth of these cells.

Apoptosis assays

Terminal deoxynucleotidyl transferase-mediated dUTP nick-end labeling (TUNEL) and caspase-3 activity assays were conducted to evaluate apoptosis. For the TUNEL assay, HLF cells (1×10^6), which were treated with 1 μM ACR alone, 5 μM LY294002 alone, or a combination of these agents for 48 hours, were stained with TUNEL methods using an In Situ Cell Death Detection Kit, Fluorescein (Roche Diagnostics, Mannheim, Germany) [25]. The caspase-3 activity assay was performed using HLF cells that were treated with the same concentrations of the test drugs for 72 hours. The cell lysates were prepared and the caspase-3 activity assay was performed using an Apoalert Caspase Fluorescent Assay Kit (Clontech Laboratories, Mountain View, CA, USA) [30].

Protein extraction and western blot analysis

Protein extracts were prepared from HLF cells treated with 1 μM ACR alone, 5 μM LY294002 alone, or a combination of these agents for 12 hours because this treatment time was appropriate for evaluating the expression levels of phosphorylated extracellular signal-regulated kinase (p-ERK), phosphorylated Akt (p-Akt), and phosphorylated RXRα (p-RXRα) proteins [25,29,30]. Equivalent amounts of extracted protein were examined by western blot analysis using specific antibodies [25]. The anti-RXRα and anti-RARβ antibodies were from Santa Cruz Biotechnology (Santa Cruz, CA, USA). The primary antibodies for ERK, p-ERK, Akt, p-Akt, and glyceraldehyde 3-phosphate dehydrogenase (GAPDH) were from Cell Signaling Technology (Beverly, MA, USA). The antibody for p-RXRα was kindly provided by Drs. S. Kojima

and H. Tatsukawa (RIKEN Advanced Science Institute, Saitama, Japan).

RNA extraction and quantitative RT-PCR analysis

Total RNA was isolated from HLF cells using an RNAqueous-4PCR kit (Ambion Applied Biosystems, Austin, TX, USA) and cDNA was amplified from 0.2 μg of total RNA using the SuperScript III Synthesis system (Invitrogen, Carlsbad, CA, USA) [32]. Quantitative real-time reverse transcription PCR (RT-PCR) analysis was performed using specific primers that amplify the RARβ, $p21^{CIP1}$, cyclin D1, and β-actin genes. The specific primer sets used have been described elsewhere [25,30].

RXRE reporter assays

HLF cells were transfected with RXR-response element (RXRE) reporter plasmids (100 ng/well in 96-well dish), which were kindly provided by the late Dr. K. Umesono (Kyoto University, Kyoto, Japan), along with p*RL-CMV* (*Renilla* luciferase, 10 ng/well in 96-well dish; Promega) as an internal standard to normalize transfection efficiency. Transfections were carried out using Lipofectamine LTX Reagent (Invitrogen). After exposure of cells to the transfection mixture for 24 hours, the cells were treated with 1 μM ACR alone, 5 μM LY294002 alone, or a combination of these agents for 24 hours. The cell lysates were then prepared, and the luciferase activity of each cell lysate was determined using a dual-luciferase reporter assay system (Promega) [25].

Statistical analysis

The data are expressed in terms of means ± SD. The statistical significance of the differences in the mean values was assessed using one-way ANOVA, followed by Tukey-Kramer multiple comparison tests. Values of <0.05 were considered significant.

Results

ACR and LY294002 cause preferential inhibition of growth in HLF human HCC cells in comparison with Hc normal hepatocytes

In the initial study, the growth inhibitory effect of ACR and LY294002 on HLF human HCC cells and on Hc hepatocytes was examined. ACR (Figure 1A) and LY294002 (Figure 1B) inhibited the growth of HLF cells with IC_{50} values of approximately 6.8 μM and 15 μM, respectively. On the other hand, Hc cells were resistant to these agents because the IC_{50} values of ACR and LY294002 for the growth inhibition of Hc cells were each greater than 50 μM (Figure 1). These results suggest that ACR and LY294002 preferentially inhibit the growth of HCC cells compared with that of normal hepatocytes.

ACR along with LY294002 causes synergistic inhibition of growth in HCC cells

Next, the effects of the combined treatment of ACR plus LY294002 on the growth of HCC-derived cells and Hc hepatocytes were examined. When HLF human HCC cells were treated with a range of concentrations of these agents, the CI indices for less than 1 μM ACR (0.5 or 1 μM) plus less than 10 μM LY294002 (5 or 10 μM) were 1+ (slight synergism), 2+ (moderate synergism), or 3+ (synergism). In particular, the combination of as little as 1 μM ACR (approx. IC_{15} value) and 5 μM LY294002 (approx. IC_{25} value) exerted synergistic growth inhibition because the CI-isobologram analysis yielded a CI index of 0.54 (3+), which indicates synergism [25,27,30,31], with this combination (Figure 2A,B, and Table 1). In other HCC cell lines, including Huh7, Hep3B, and HepG2 cell lines, similar findings were also obtained using Huh7 and Hep3B cells; the combination of 1 μM ACR plus 5 μM LY294002 significantly suppressed the growth of these cells (Figure 2C). In contrast, the growth of Hc normal hepatocytes was not affected by the combination of these agents; even a

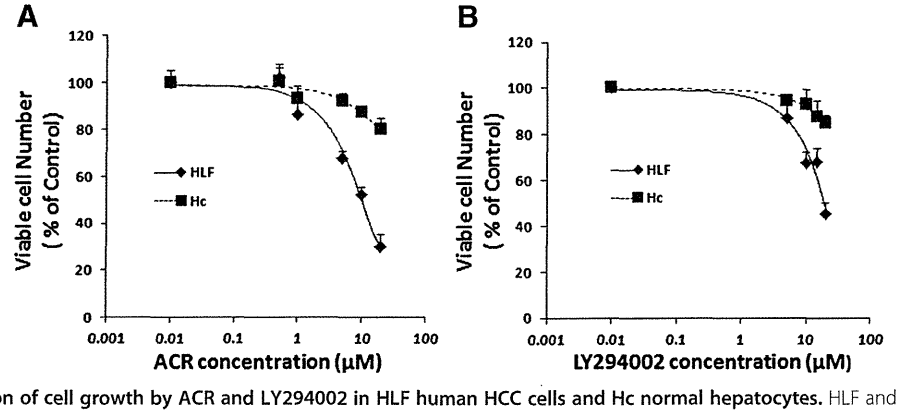

Figure 1 Inhibition of cell growth by ACR and LY294002 in HLF human HCC cells and Hc normal hepatocytes. HLF and Hc cells were treated with the indicated concentrations of ACR **(A)** or LY294002 **(B)** for 48 hours. Cell viability was determined by the MTS assay and expressed as a percentage of the control value. Error bars present the SD of triplicate assays.

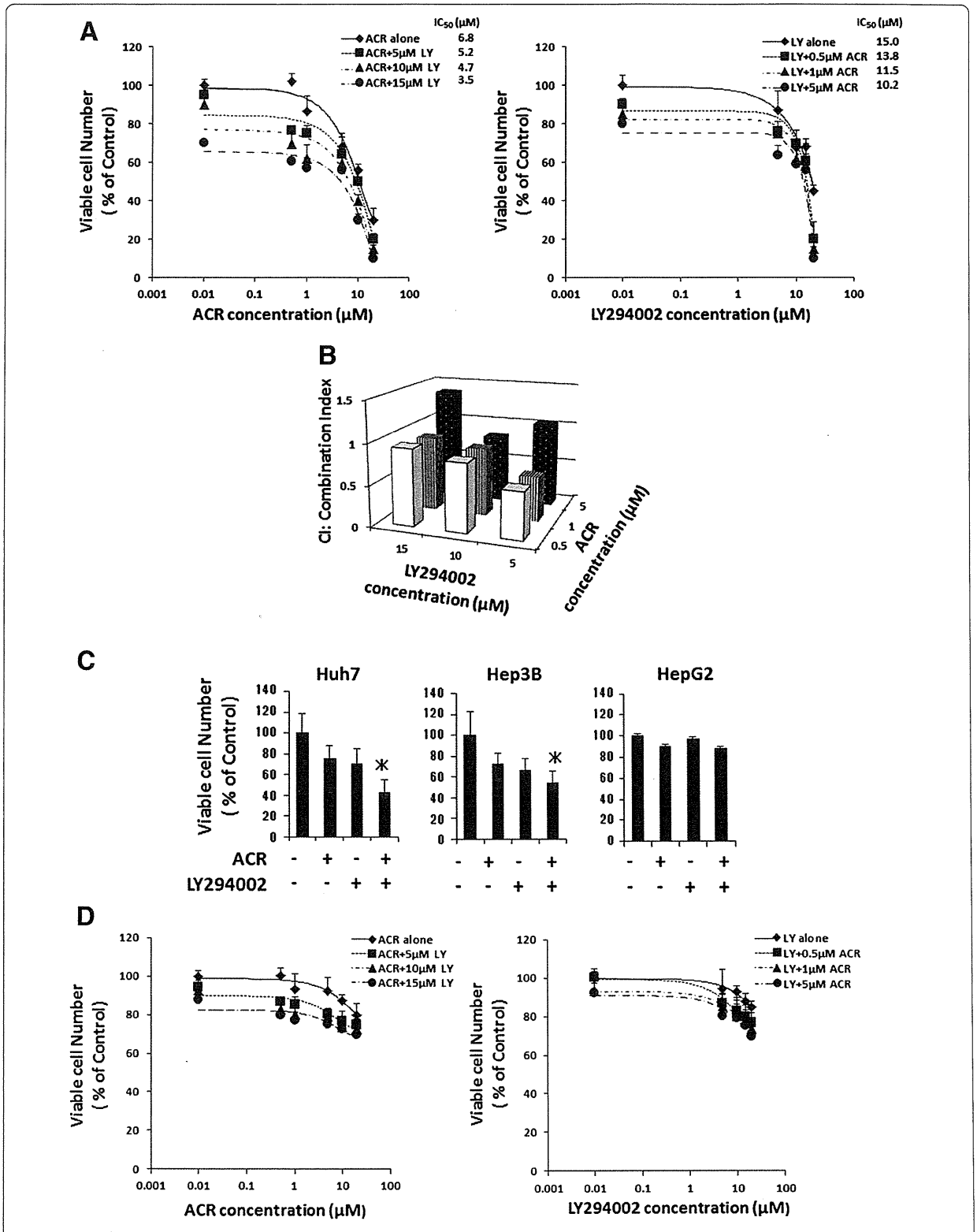

Figure 2 (See legend on next page.)

(See figure on previous page.)
Figure 2 Inhibition of cell growth by ACR alone, LY294002 alone, or various combinations of these agents in human HCC-derived cells and Hc normal hepatocytes. (A) HLF human HCC cells were treated with the indicated concentrations of ACR alone, LY294002 alone, and various combinations of these agents for 48 hours. **(B)** The data obtained in **(A)** was used to calculate the combination index. **(C)** Huh7, Hep3B, and HepG2 human HCC cells were treated with vehicle, 1 μM ACR alone, 5 μM LY294002 alone, or a combination of 1 μM ACR and 5 μM LY294002 for 48 hours. **(D)** Hc human hepatocytes were treated with the indicated concentrations of ACR alone, LY294002 alone, and various combinations of these agents for 48 hours. **(A)**, **(C)**, and **(D)** Cell viability was determined by the MTS assay and expressed as a percentage of the control value. Error bars present the SD of triplicate assays. * $P < 0.05$.

combination of high concentrations of ACR (5 μM) plus LY294002 (15 μM) did not inhibit the growth of Hc cells in the present study (Figure 2D).

ACR plus BKM120 cause synergistic inhibition of growth in HLF cells

In order to examine whether PI3K inhibitors are promising agents to potently suppress the growth of HCC cells in conjunction with ACR, the combined effects of ACR plus BKM120, another selective PI3K inhibitor [33], on the growth of HLF cells were next investigated. The combination of ACR plus BKM120 significantly inhibited the growth of HLF cells. In particular, when the cells were treated with 1 μM ACR plus 5 μM BKM120, the CI-isobologram analysis yielded a CI-index of 3+ (synergism) (Figure 3A,B, and Table 1). These findings suggest that combination therapy using ACR plus PI3K inhibitors might be an effective regimen for inhibiting the growth of HCC cells.

ACR plus LY294002 cooperatively induce apoptosis in HLF cells

The next study examined whether the synergistic growth inhibition in HLF cells induced by treatment with ACR plus LY294002 is associated with the induction of apoptosis. The ratio of TUNEL-positive cells was not significantly increased by treatment with 1 μM ACR alone (26.9%) or 5 μM LY294002 alone (27.6%) in comparison to that of control untreated cells (15.2%). However, when the cells were treated with the combination of these agents, TUNEL-positive cells significantly increased to 54.4% of the total remaining cells (Figure 4A). Similar results were also observed in the caspase-3 activity assay; the combined treatment with ACR plus LY294002 significantly increased the levels of caspase-3 activity in HLF cells, whereas treatment with ACR alone or LY294002 alone did not exert such an effect (Figure 4B).

ACR plus LY294002 cooperatively suppress the phosphorylation of RXRα, ERK, and Akt and increase the RXRE promoter activity in HLF cells

RXRα phosphorylation is involved in the development of HCC, and thus might be a promising target for HCC chemoprevention [4-9]. Therefore, the effects of the combination of ACR and LY294002 on the phosphorylation of RXRα and related signaling molecules were next investigated in HLF cells. As shown in Figure 5A, there was a significant decrease in the expression levels of p-RXRα, p-ERK, and p-Akt proteins when the cells were treated with 1 μM ACR. Treatment with 5 μM LY294002 also caused a marked decrease in the expression levels of p-RXRα and p-Akt proteins in these cells. Moreover, the decrease in the expression levels of p-RXRα, p-ERK, and p-Akt proteins was greater when the cells were treated with a combination of these agents.

Table 1 Combined effects of ACR and PI3K inhibitors on HLF cells

ACR concentration (μM)	LY294002 concentration (μM)			BKM120 concentration (μM)		
	5	10	15	5	10	15
0.5	+++	+	±	±	++	++
1	+++	++	±	+++	++	+
5	-	++	-	-	-	-

Note:
"-", CI1.1-1.3 moderate antagonism;
"±", CI0.9-1.1 additive effect;
"+", CI0.8-0.9 slight synergism;
"++", CI0.6-0.8 moderate synergism;
"+++", CI0.4-0.6 synergism;
Abbreviations: CI Combination index, ACR Acyclic retinoid.

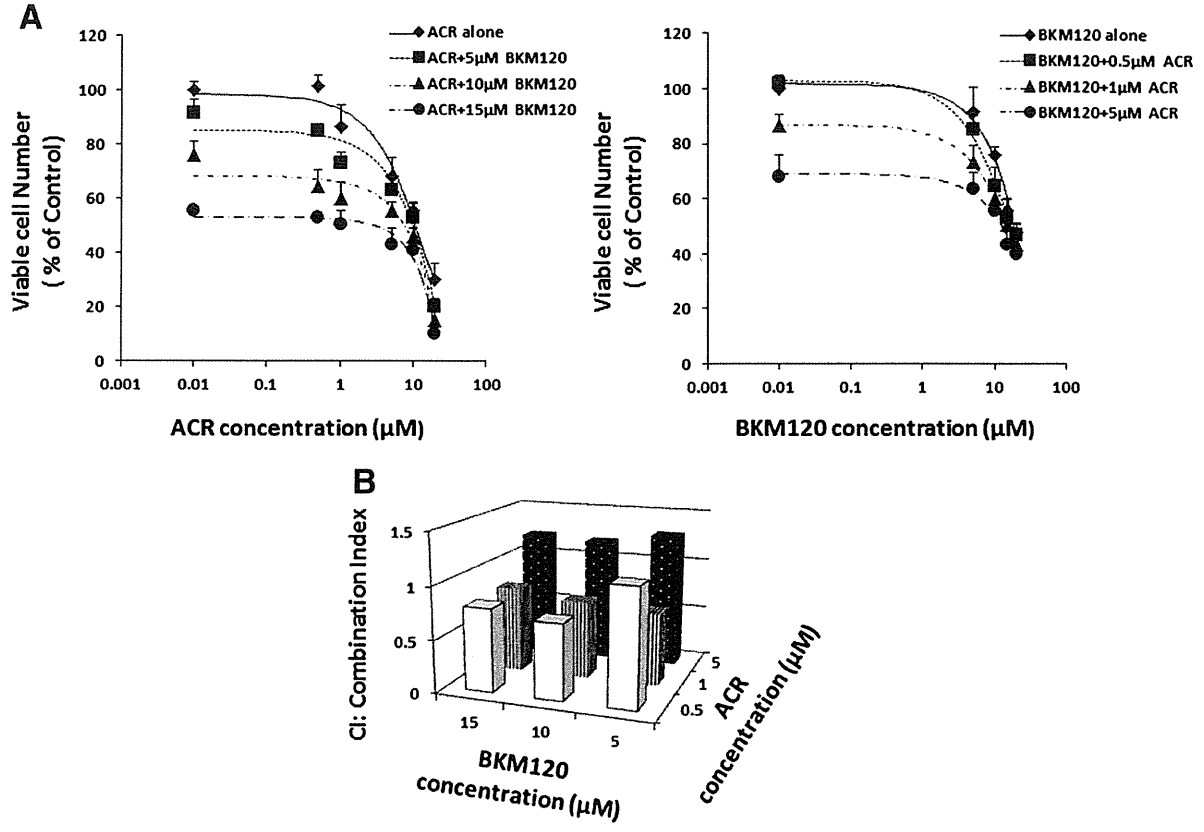

Figure 3 Inhibition of cell growth by ACR alone, BKM120 alone, or various combinations of these agents in HCC cells. (A) HLF human HCC cells were treated with the indicated concentrations of ACR alone, BKM120 alone, or various combinations of these agents for 48 hours. Cell viability was determined by the MTS assay and expressed as a percentage of the control value. **(B)** The data obtained in **(A)** was used to calculate the combination index. Error bars present the SD of triplicate assays.

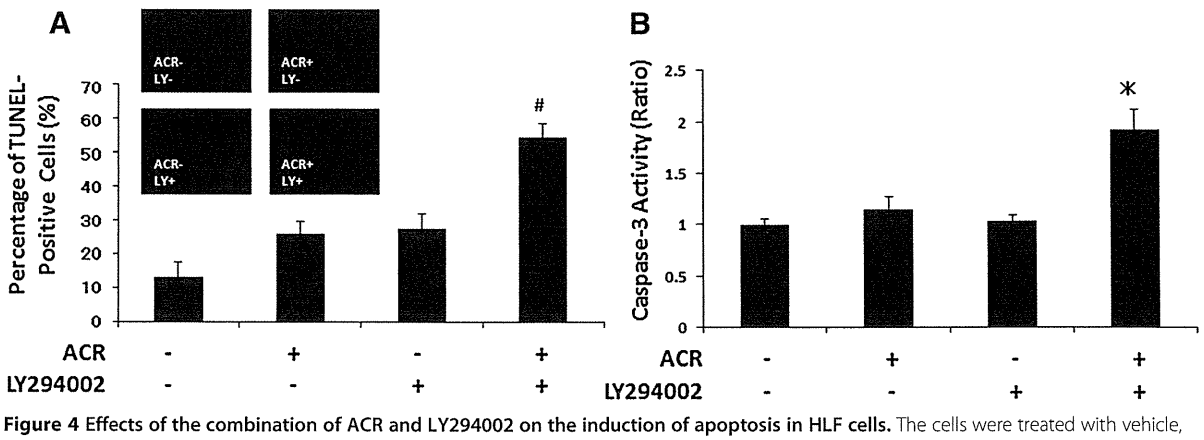

Figure 4 Effects of the combination of ACR and LY294002 on the induction of apoptosis in HLF cells. The cells were treated with vehicle, 1 μM ACR alone, 5 μM LY294002 alone, or a combination of 1 μM ACR and 5 μM LY294002 for 48 or 72 hours. **(A)** TUNEL assays were performed using cells treated with test drugs for 48 hours. TUNEL-positive cells were counted and examined as the percentage of the DAPI-positive cell number (500 cells were counted in each flask). **(B)** Caspase-3 activity assays were performed with a fluorometric system using samples treated for 72 hours. # $P < 0.01$. * $P < 0.05$.

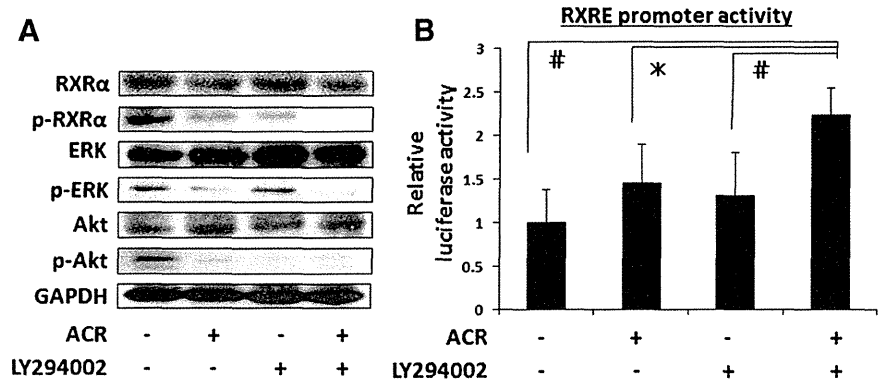

Figure 5 Effects of the combination of ACR and LY294002 on the phosphorylation of RXRα, ERK, and Akt proteins and the transcriptional activity of the RXRE promoter in HLF cells. (A) The cells were treated with vehicle, 1 μM ACR alone, 5 μM LY294002 alone, or a combination of 1 μM ACR and 5 μM LY294002 for 12 hours. The extracted proteins were examined by western blot analysis using the respective antibodies. Repeat western blots gave similar results. **(B)** A transient transfection reporter assay was performed with the RXRE luciferase reporter in the presence of vehicle, 1 μM ACR alone, 5 μM LY294002 alone, or a combination of 1 μM ACR and 5 μM LY294002. Relative luciferase activity was determined after 24 hours. Columns and lines indicate the means and SD of triplicate assays. # $P < 0.01$. * $P < 0.05$.

In addition, there was a significant increase in the transcriptional activity of the RXRE reporter when HLF cells were treated with a combination of ACR and LY294002, whereas treatment with the same concentrations of ACR alone or LY294002 alone did not upregulate the activity of this promoter (Figure 5B). Because RXRs modulate the expression of target genes by interacting with the RXRE element located in the promoter regions of these genes [1,2], this finding may indicate that LY294002 enhances the transcriptional activity of the RXRE promoter induced by ACR, at least in part by inhibiting the phosphorylation of RXRα.

ACR and LY294002 cooperatively increase the cellular levels of RARβ and $p21^{CIP1}$, but decrease the levels of cyclin D1, in HLF cells

Because the transcriptional activity of the RXRE promoter was significantly increased by treatment with ACR plus LY294002 (Figure 5B), the next study examined whether this combination cooperatively altered the expression of target molecules of ACR, including RARβ, $p21^{CIP1}$, and cyclin D1 [13,25,27,34], in HLF cells. As shown in Figure 6A, the mRNA and protein expression levels of RARβ were significantly increased on combined treatment with ACR and LY294002. Quantitative RT-PCR analyses also revealed that there was a significant increase in the levels of $p21^{CIP1}$ mRNA, but a decrease in the levels of cyclin D1 mRNA, in HLF cells, upon treatment with this combination (Figure 6B).

Discussion and conclusions

In order to improve the clinical outcome for patients with HCC, development of effective strategies for the chemoprevention and chemotherapy of this malignancy is urgently required. We believe that combination chemoprevention using ACR as a key agent is a promising method for attaining this objective, because it provides an opportunity to take advantage of the synergistic effects of ACR on growth inhibition in HCC cells [17,25-30]. The present study provides the first evidence that the combination of ACR with LY294002, a PI3K inhibitor, synergistically inhibited the growth of human HCC cells through the induction of apoptosis. Activation of the PI3K/Akt pathway, which is common in many cancers such as HCC [21,22], contributes to the inhibition of apoptosis and induction of therapeutic resistance in cancer cells, indicating that targeting this pathway can inhibit the survival and growth of cancer cells through various mechanisms such as potentiation of the effects of chemotherapeutic drugs [18-20,23,24]. For instance, the combination of all-*trans* retinoic acid with LY294002 enhanced growth suppressive effects in leukemic cells by inducing apoptosis [35].

The hypotheses that explain the synergism generated by the combination of ACR and LY294002 are summarized in Figure 7. First, it should be noted that phosphorylation of RXRα was markedly inhibited by the combination of ACR and LY294002 in the present study. This finding seems to be significant because RXRα phosphorylation plays a role in the development of HCC and, therefore, might be a critical target for the implementation of HCC chemoprevention [5,7-9]. Accumulation of phosphorylated RXRα induced by the Ras/MAPK activation interferes with the function of normal (unphosphorylated) RXRα in a dominant negative manner [8,9]. This and prior studies [4,17,25,28] show that ACR alone inhibits the phosphorylation of RXRα and ERK proteins in HCC cells. Moreover, in the present study, ACR alone also dephosphorylated the Akt protein in HLF cells. These

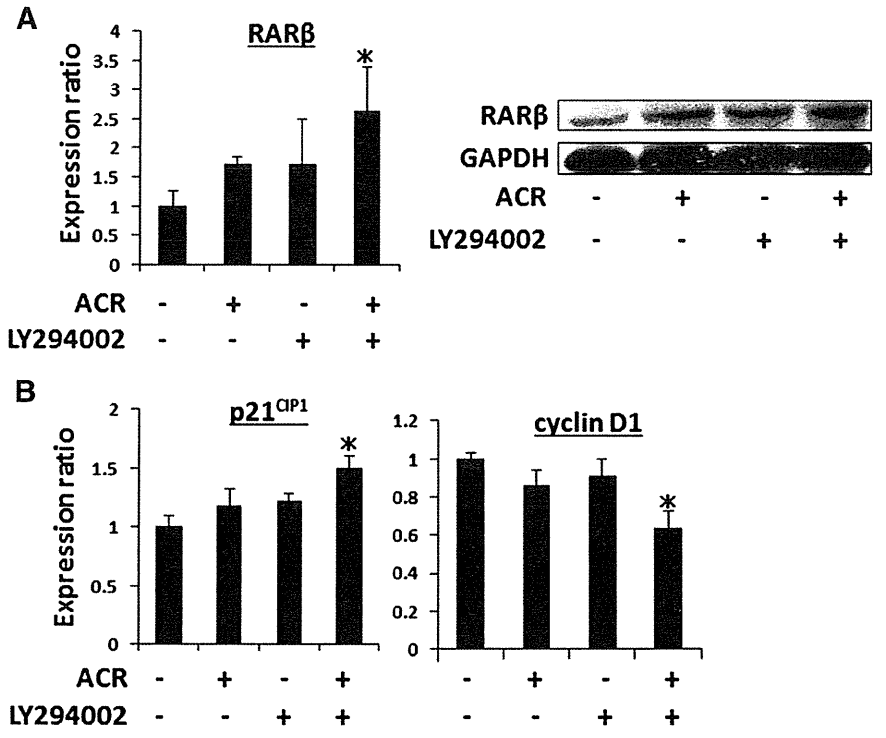

Figure 6 Effects of the combination of ACR and LY294002 on the cellular expression levels of RARβ, $p21^{CIP1}$, and cyclin D1 in HLF cells. **(A)** The expression levels of RARβ mRNA (left panel) and protein (right panel) were examined by quantitative real-time RT-PCR analysis and western blot analysis, respectively, using cells treated with the test drugs for 24 hours. **(B)** Quantitative real-time RT-PCR analysis to examine the expression levels of $p21^{CIP1}$ and cyclin D1 mRNAs were performed using cells treated with the test drugs for 24 hours. The expression level of each mRNA was normalized to the level of β-actin mRNA. Values represent the means ± SD of triplicate analyses. * $P < 0.05$.

findings suggest that the combination of ACR and LY294002 cooperatively inhibit the phosphorylation of RXRα through dephosphorylation of ERK and Akt, which leads to the synergistic inhibition of growth and the induction of apoptosis in HCC cells. The results of the present research, together with those of previous studies [17,25,28-30], suggest that dephosphorylation of RXRα might be a key mechanism for ACR-based combination chemoprevention in HCC cells.

Phosphorylated RXRα loses its ability to form heterodimers with RARβ and this is associated with resistance to retinoids [7]. Therefore, restoration of the function of RXRα by inhibiting its phosphorylation is critical to regulate the expression of retinoid target genes [4-9]. In comparison to treatment with ACR alone or LY294002 alone, combined treatment with these agents significantly increased the transcriptional activity of the RXRE reporter in the present study. This combination also significantly altered the expression levels of ACR target genes, such as RARβ, $p21^{CIP1}$, and cyclin D1 mRNA [13,25,27,34]. Particularly, the induction of RARβ by the combination of ACR and LY294002 might play a crucial role in inhibiting the growth of HCC cells because RARβ, which is a receptor for ACR [36], can exert tumor-suppressive effects in cancer cells and thus be considered as a tumor suppressor gene [37].

In this study, the phosphorylation of Akt is inhibited by ACR alone in HLF cells. This finding seems to be of interest because Akt phosphorylation plays a critical role in cell survival, prevention of apoptosis, and progression of cell cycle in various types of tumors, including HCC [21,22]. The precise mechanism by which ACR inhibits the phosphorylation of Akt protein has not been determined. However, we assume that the dephosphorylation of this protein by ACR might be explained by, at least in part, its ability to inhibit growth factor-dependent RTK activity, because Akt is potently phosphorylated by the activation of RTKs [8,9,14,15,18-20]. For instance, ACR inhibits the growth of HCC cells and prevents chemically induced liver tumorigenesis by targeting the transforming growth factor-α/epidermal growth factor receptor (EGFR) axis, which belongs to RTKs [14,15]. Moreover, a recent study showed that retinol inhibited PI3K activity by decreasing the interaction between PI3K and phosphatidylinositol and this was associated with suppression of cell growth in colon cancer cells [38]. These studies suggest that the PI3K/Akt signaling pathway might be a critical target for retinoids to exert their anti-cancer and chemopreventive properties.

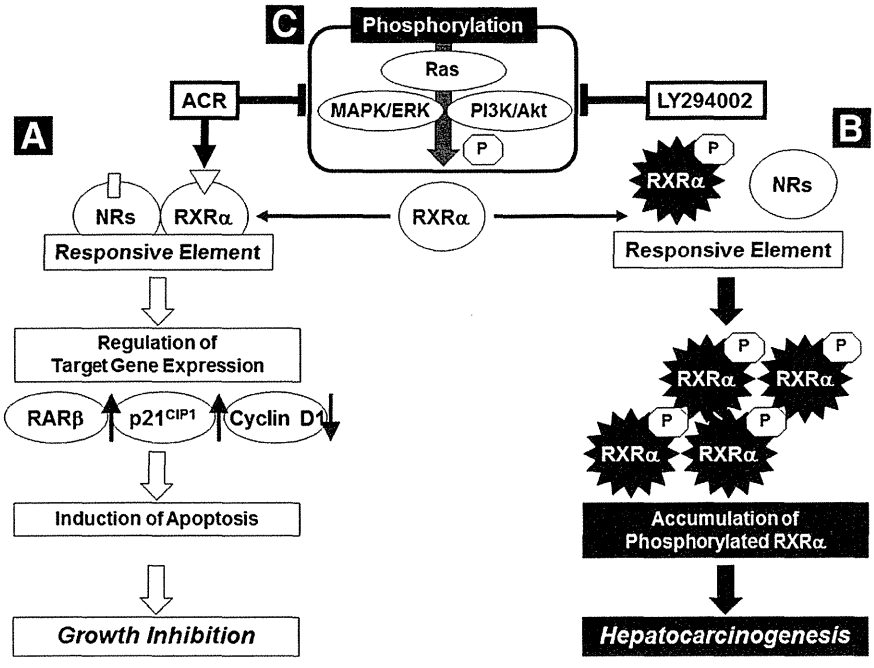

Figure 7 A hypothetical schematic representation of the effects of the combination of ACR and LY294002 on growth inhibition in HCC cells. When ACR binds to and activates RXRα, it forms homo- and/or heterodimers with other nuclear receptors (NRs), including RARs. This results in the activation of the transcriptional activity of the responsive element, thus controlling the expression of the target genes, such as RARβ, $p21^{CIP1}$, and cyclin D1, which induce apoptosis and inhibit the growth of HCC cells **(A)**. In HCC cells, the MAPK/ERK and PI3K/Akt pathways, both of which are located downstream of Ras, are highly activated and phosphorylate the RXRα protein. The accumulation of phosphorylated RXRα protein, which impairs dimer formation and the subsequent transactivation functions of this receptor, cause a deviation from normal cell proliferation and differentiation, thereby playing a critical role in liver carcinogenesis **(B)**. ACR and LY294002 inhibit RXRα phosphorylation by inhibiting ERK and Akt phosphorylation, resulting in restoration of receptor function and activation of the transcriptional activity of the responsive element **(C)**. For additional details, see the Discussion section.

In the current study, the combination of ACR and LY294002 significantly inhibited the growth of HLF, Huh7, and Hep3B HCC cells, whereas the growth of HepG2 cells, the other HCC cell line, was not suppressed by this combination. This might be associated with the phosphorylation status of ERK and Akt proteins because the expression levels of p-ERK and p-Akt proteins were increased in HLF, Huh7, and Hep3B cells compared with HepG2 cells [29]. These results, on the other hand, suggest that HCC cells that overexpress p-ERK and p-Akt proteins might be more sensitive targets for combination therapy using ACR and PI3K inhibitors.

Finally, it should be emphasized that combination therapy and prevention are advantageous because, in addition to providing the potential for synergistic effects, they may reduce the opportunity for the development of drug resistance by cancer cells. Several preclinical studies have shown that cancer cells harboring activated Ras mutations appear to be resistant to treatment with PI3K inhibitor alone [23,39]. However, the use of a combination of the PI3K/Akt inhibitor and a MAPK inhibitor significantly exerted anti-cancer effects in *Kars* G12D-driven or EGFR-mutant lung tumors [23,24]. These studies suggest that effective treatment with PI3K inhibitors require concomitant therapies that target RTK/Ras/MAPK signaling and, therefore, ACR, which can inhibit this signaling pathway [8,9,14,15,40], might be a preferable partner for PI3K inhibitors.

In conclusion, the present study indicates that the combination of ACR and LY294002, which can inhibit the phosphorylation of RXRα, causes a synergistic induction of apoptosis and inhibition of cell growth in human HCC cells. The results of our study suggest that this combination might hold promise as a clinical modality for the prevention and treatment of HCC, due to their synergistic effects. In particular, our finding that the combination regimen using 1 μM ACR plus 5 μM LY294002 synergistically inhibits the growth of HCC cells seems to be clinically relevant because this concentration (1 μM) is approximately the same as the plasma concentration of ACR (which ranged from 1 to 5 μM) in a clinical trial that demonstrated the chemopreventive effects of this agent in the recurrence of secondary HCC [10,11].

Abbreviations

ACR: Acyclic retinoid; CI: Combination index; DMEM: Dulbecco's modified eagle medium; EGFR: Epidermal growth factor receptor; ERK: Extracellular signal-regulated kinase; GAPDH: Glyceraldehyde 3-phosphate dehydrogenase; HCC: Hepatocellular carcinoma; IFN: Interferon; MAPK: Mitogen-activated protein kinase; PI3K: Phosphatidylinositol 3-kinase; RAR: Retinoic acid receptor; RTK: Receptor tyrosine kinase; RT-PCR: Reverse transcription PCR; RXR: Retinoid X receptor; RXRE: Retinoid X receptor response element; TUNEL: Terminal deoxynucleotidyl transferase-mediated dUTP nick-end labeling.

Competing interests

The authors declare that they have no competing interests.

Authors' contributions

AB, MS, and TO conceived of the study, participated in its design, and drafted the manuscript. AB, MS, TO, YS, MK, and TK performed in vitro experiment. DT performed statistical analysis. HT and HM helped to draft the manuscript. All authors read and approved the final manuscript.

Acknowledgements

This work was supported in part by Grants-in-Aid from the Ministry of Education, Science, Sports and Culture of Japan (No. 22790638 to M. S. and No. 21590838 to H. M.) and by a Grant-in-Aid for the 3rd Term Comprehensive 10-Year Strategy for Cancer Control from the Ministry of Health, Labour and Welfare of Japan.

Received: 28 May 2013 Accepted: 3 October 2013
Published: 8 October 2013

References

1. Mangelsdorf DJ, Thummel C, Beato M, Herrlich P, Schutz G, Umesono K, Blumberg B, Kastner P, Mark M, Chambon P, Evans RM: **The nuclear receptor superfamily: the second decade.** *Cell* 1995, **83**:835–839.
2. Chambon P: **A decade of molecular biology of retinoic acid receptors.** *FASEB J* 1996, **10**:940–954.
3. Altucci L, Leibowitz MD, Ogilvie KM, de Lera AR, Gronemeyer H: **RAR and RXR modulation in cancer and metabolic disease.** *Nat Rev Drug Discov* 2007, **6**:793–810.
4. Matsushima-Nishiwaki R, Okuno M, Takano Y, Kojima S, Friedman SL, Moriwaki H: **Molecular mechanism for growth suppression of human hepatocellular carcinoma cells by acyclic retinoid.** *Carcinogenesis* 2003, **24**:1353–1359.
5. Matsushima-Nishiwaki R, Okuno M, Adachi S, Sano T, Akita K, Moriwaki H, Friedman SL, Kojima S: **Phosphorylation of retinoid X receptor alpha at serine 260 impairs its metabolism and function in human hepatocellular carcinoma.** *Cancer Res* 2001, **61**:7675–7682.
6. Adachi S, Okuno M, Matsushima-Nishiwaki R, Takano Y, Kojima S, Friedman SL, Moriwaki H, Okano Y: **Phosphorylation of retinoid X receptor suppresses its ubiquitination in human hepatocellular carcinoma.** *Hepatology* 2002, **35**:332–340.
7. Yoshimura K, Muto Y, Shimizu M, Matsushima-Nishiwaki R, Okuno M, Takano Y, Tsurumi H, Kojima S, Okano Y, Moriwaki H: **Phosphorylated retinoid X receptor alpha loses its heterodimeric activity with retinoic acid receptor beta.** *Cancer Sci* 2007, **98**:1868–1874.
8. Shimizu M, Takai K, Moriwaki H: **Strategy and mechanism for the prevention of hepatocellular carcinoma: phosphorylated retinoid X receptor alpha is a critical target for hepatocellular carcinoma chemoprevention.** *Cancer Sci* 2009, **100**:369–374.
9. Shimizu M, Sakai H, Moriwaki H: **Chemoprevention of hepatocellular carcinoma by acyclic retinoid.** *Front Biosci* 2011, **16**:759–769.
10. Muto Y, Moriwaki H, Ninomiya M, Adachi S, Saito A, Takasaki KT, Tanaka T, Tsurumi K, Okuno M, Tomita E, Nakamura T, Kojima T: **Prevention of second primary tumors by an acyclic retinoid, polyprenoic acid, in patients with hepatocellular carcinoma. Hepatoma prevention study group.** *N Engl J Med* 1996, **334**:1561–1567.
11. Muto Y, Moriwaki H, Saito A: **Prevention of second primary tumors by an acyclic retinoid in patients with hepatocellular carcinoma.** *N Engl J Med* 1999, **340**:1046–1047.
12. Suzui M, Masuda M, Lim JT, Albanese C, Pestell RG, Weinstein IB: **Growth inhibition of human hepatoma cells by acyclic retinoid is associated with induction of p21(CIP1) and inhibition of expression of cyclin D1.** *Cancer Res* 2002, **62**:3997–4006.
13. Suzui M, Shimizu M, Masuda M, Lim JT, Yoshimi N, Weinstein IB: **Acyclic retinoid activates retinoic acid receptor beta and induces transcriptional activation of p21(CIP1) in HepG2 human hepatoma cells.** *Mol Cancer Ther* 2004, **3**:309–316.
14. Nakamura N, Shidoji Y, Moriwaki H, Muto Y: **Apoptosis in human hepatoma cell line induced by 4,5-didehydro geranylgeranoic acid (acyclic retinoid) via down-regulation of transforming growth factor-alpha.** *Biochem Biophys Res Commun* 1996, **219**:100–104.
15. Kagawa M, Sano T, Ishibashi N, Hashimoto M, Okuno M, Moriwaki H, Suzuki R, Kohno H, Tanaka T: **An acyclic retinoid, NIK-333, inhibits N-diethylnitrosamine-induced rat hepatocarcinogenesis through suppression of TGF-alpha expression and cell proliferation.** *Carcinogenesis* 2004, **25**:979–985.
16. Shimizu M, Sakai H, Shirakami Y, Iwasa J, Yasuda Y, Kubota M, Takai K, Tsurumi H, Tanaka T, Moriwaki H: **Acyclic retinoid inhibits diethylnitrosamine-induced liver tumorigenesis in obese and diabetic C57BLKS/J- + (db)/+Lepr(db) mice.** *Cancer Prev Res* 2011, **4**:128–136.
17. Shimizu M, Shirakami Y, Sakai H, Iwasa J, Shiraki M, Takai K, Naiki T, Moriwaki H: **Combination of acyclic retinoid with branched-chain amino acids inhibits xenograft growth of human hepatoma cells in nude mice.** *Hepatol Res* 2012, **42**:1241–1247.
18. Engelman JA: **Targeting PI3K signalling in cancer: opportunities, challenges and limitations.** *Nat Rev Cancer* 2009, **9**:550–562.
19. Courtney KD, Corcoran RB, Engelman JA: **The PI3K pathway as drug target in human cancer.** *J Clin Oncol* 2010, **28**:1075–1083.
20. Vivanco I, Sawyers CL: **The phosphatidylinositol 3-Kinase AKT pathway in human cancer.** *Nat Rev Cancer* 2002, **2**:489–501.
21. Zhou Q, Lui VW, Yeo W: **Targeting the PI3K/Akt/mTOR pathway in hepatocellular carcinoma.** *Future Oncol* 2011, **7**:1149–1167.
22. Llovet JM, Bruix J: **Molecular targeted therapies in hepatocellular carcinoma.** *Hepatology* 2008, **48**:1312–1327.
23. Engelman JA, Chen L, Tan X, Crosby K, Guimaraes AR, Upadhyay R, Maira M, McNamara K, Perera SA, Song Y, Chirieac LR, Kaur R, Lightbown A, Simendinger J, Li T, Padera RF, Garcia-Echeverria C, Weissleder R, Mahmood U, Cantley LC, Wong KK: **Effective use of PI3K and MEK inhibitors to treat mutant Kras G12D and PIK3CA H1047R murine lung cancers.** *Nat Med* 2008, **14**:1351–1356.
24. Faber AC, Li D, Song Y, Liang MC, Yeap BY, Bronson RT, Lifshits E, Chen Z, Maira SM, Garcia-Echeverria C, Wong KK, Engelman JA: **Differential induction of apoptosis in HER2 and EGFR addicted cancers following PI3K inhibition.** *Proc Natl Acad Sci U S A* 2009, **106**:19503–19508.
25. Tatebe H, Shimizu M, Shirakami Y, Sakai H, Yasuda Y, Tsurumi H, Moriwaki H: **Acyclic retinoid synergises with valproic acid to inhibit growth in human hepatocellular carcinoma cells.** *Cancer Lett* 2009, **285**:210–217.
26. Obora A, Shiratori Y, Okuno M, Adachi S, Takano Y, Matsushima-Nishiwaki R, Yasuda I, Yamada Y, Akita K, Sano T, Shimada J, Kojima S, Okano Y, Friedman SL, Moriwaki H: **Synergistic induction of apoptosis by acyclic retinoid and interferon-beta in human hepatocellular carcinoma cells.** *Hepatology* 2002, **36**:1115–1124.
27. Shimizu M, Suzui M, Deguchi A, Lim JT, Xiao D, Hayes JH, Papadopoulos KP, Weinstein IB: **Synergistic effects of acyclic retinoid and OSI-461 on growth inhibition and gene expression in human hepatoma cells.** *Clin Cancer Res* 2004, **10**:6710–6721.
28. Kanamori T, Shimizu M, Okuno M, Matsushima-Nishiwaki R, Tsurumi H, Kojima S, Moriwaki H: **Synergistic growth inhibition by acyclic retinoid and vitamin K2 in human hepatocellular carcinoma cells.** *Cancer Sci* 2007, **98**:431–437.
29. Tatebe H, Shimizu M, Shirakami Y, Tsurumi H, Moriwaki H: **Synergistic growth inhibition by 9-cis-retinoic acid plus trastuzumab in human hepatocellular carcinoma cells.** *Clin Cancer Res* 2008, **14**:2806–2812.
30. Ohno T, Shirakami Y, Shimizu M, Kubota M, Sakai H, Yasuda Y, Kochi T, Tsurumi H, Moriwaki H: **Synergistic growth inhibition of human hepatocellular carcinoma cells by acyclic retinoid and GW4064, a farnesoid X receptor ligand.** *Cancer Lett* 2012, **323**:215–222.
31. Zhao L, Wientjes MG, Au JL: **Evaluation of combination chemotherapy: integration of nonlinear regression, curve shift, isobologram, and combination index analyses.** *Clin Cancer Res* 2004, **10**:7994–8004.
32. Shimizu M, Yasuda Y, Sakai H, Kubota M, Terakura D, Baba A, Ohno T, Kochi T, Tsurumi H, Tanaka T, Moriwaki H: **Pitavastatin suppresses diethylnitrosamine-induced liver preneoplasms in male C57BL/KsJ-db/db obese mice.** *BMC Cancer* 2011, **11**:281.
33. Kirstein MM, Boukouris AE, Pothiraju D, Buitrago-Molina LE, Marhenke S, Schutt J, Orlik J, Kühnel F, Hegermann J, Manns MP, Vogel A: **Activity of the mTOR**

inhibitor RAD001, the dual mTOR and PI3-kinase inhibitor BEZ235 and the PI3-kinase inhibitor BKM120 in hepatocellular carcinoma. *Liver Int* 2013, **33**:780–793.
34. Shimizu M, Suzui M, Deguchi A, Lim JT, Weinstein IB: **Effects of acyclic retinoid on growth, cell cycle control, epidermal growth factor receptor signaling, and gene expression in human squamous cell carcinoma cells.** *Clin Cancer Res* 2004, **10**:1130–1140.
35. Zhao S, Konopleva M, Cabreira-Hansen M, Xie Z, Hu W, Milella M, Estrov Z, Mills GB, Andreeff M: **Inhibition of phosphatidylinositol 3-kinase dephosphorylates BAD and promotes apoptosis in myeloid leukemias.** *Leukemia* 2004, **18**:267–275.
36. Yamada Y, Shidoji Y, Fukutomi Y, Ishikawa T, Kaneko T, Nakagama H, Imawari M, Moriwaki H, Muto Y: **Positive and negative regulations of albumin gene expression by retinoids in human hepatoma cell lines.** *Mol Carcinog* 1994, **10**:151–158.
37. Alvarez S, Germain P, Alvarez R, Rodriguez-Barrios F, Gronemeyer H, de Lera AR: **Structure, function and modulation of retinoic acid receptor beta, a tumor suppressor.** *Int J Biochem Cell Biol* 2007, **39**:1406–1415.
38. Park EY, Wilder ET, Chipuk JE, Lane MA: **Retinol decreases phosphatidylinositol 3-kinase activity in colon cancer cells.** *Mol Carcinog* 2008, **47**:264–274.
39. Ihle NT, Lemos R Jr, Wipf P, Yacoub A, Mitchell C, Siwak D, Mills GB, Dent P, Kirkpatrick DL, Powis G: **Mutations in the phosphatidylinositol-3-kinase pathway predict for antitumor activity of the inhibitor PX-866 whereas oncogenic Ras is a dominant predictor for resistance.** *Cancer Res* 2009, **69**:143–150.
40. Nakagawa T, Shimizu M, Shirakami Y, Tatebe H, Yasuda I, Tsurumi H, Moriwaki H: **Synergistic effects of acyclic retinoid and gemcitabine on growth inhibition in pancreatic cancer cells.** *Cancer Lett* 2009, **273**:250–256.

doi:10.1186/1471-2407-13-465
Cite this article as: Baba *et al.*: Synergistic growth inhibition by acyclic retinoid and phosphatidylinositol 3-kinase inhibitor in human hepatoma cells. *BMC Cancer* 2013 **13**:465.

Hepatology Research

Hepatology Research 2013; 43: 459–466 doi: 10.1111/j.1872-034X.2012.01097.x

Original Article

Effects of branched-chain amino acid granules on serum albumin level and prognosis are dependent on treatment adherence in patients with liver cirrhosis

Koichi Takaguchi,[1] Hisataka Moriwaki,[2] Hisashi Doyama,[3] Masayuki Iida,[4] Michiyasu Yagura,[5] Noritomo Shimada,[8] Masahiro Kang,[9] Haruki Yamada[6] and Hiromitsu Kumada[7]

[1]Department of Hepatology, Kagawa Prefectural Central Hospital, Kagawa, [2]Department of Medicine, Gifu University Graduate School of Medicine, Gifu, [3]Department of Gastroenterology, Ishikawa Prefectural Central Hospital, Kanazawa, [4]Department of Internal Medicine, Nagoya Midori Municipal Hospital, Nagoya, [5]Department of Gastroenterology, National Hospital Organization Tokyo National Hospital, [6]Department of Internal Medicine, Social Insurance Chuo General Hospital, [7]Department of Hepatology, Toranomon Hospital, Tokyo, [8]Department of Internal Medicine, Medical Plaza Heiwadai Hospital, Chiba, and [9]Department of Internal Medicine, Sato Daiichi Hospital, Oita, Japan

Aim: To test if the treatment adherence to branched-chain amino acid (BCAA) granules influences the serum albumin level and prognosis in prospective 2984 patients with decompensated liver cirrhosis who were prescribed BCAA granules containing 952 mg of L-isoleucine, 1904 mg of L-leucine and 1144 mg of L-valine at 4.15 g/sachet three times a day after meals.

Methods: The primary end-point was the time to the event defined as "hospital admission due to progression of hepatic failure", and factors affecting this outcome were explored. Changes in serum albumin level were evaluated as the secondary end-point.

Results: Patients were divided into the good adherence group (those who reported to have taken "nearly all" prescribed doses) and the poor adherence group (those who reported to have taken "approximately half" or "less" doses), because such stratification was validated by treatment responses in plasma BCAA/tyrosine ratio. Factors related to the primary end-point were age, drug adherence during 6 months of study treatment, previous hepatic cancer, current clinical manifestations, previous clinical manifestations, baseline serum albumin level, platelet count and total bilirubin level. The cumulative event-free survival was significantly higher in the good adherence group. Increase in the serum albumin level was also greater in the good adherence group.

Conclusion: Higher BCAA treatment adherence better raised the serum albumin level, leading to improvement of event-free survival. These results indicate the importance of patient instruction for the adequate use of BCAA granules.

Key words: branched-chain amino acids, hepatic failure, liver cirrhosis, prognosis, serum albumin, treatment adherence

INTRODUCTION

ALTHOUGH LIVER CIRRHOSIS is caused by any of a wide variety of etiologies,[1] clinical features of the disease share complications such as ascites, edema, hepatic encephalopathy and esophageal varices.[2] Some of these complications are attributable to decreased serum concentrations of albumin and other proteins,[3–5] and oral supplemental branched-chain amino acid (BCAA) therapy with BCAA granules or BCAA-enriched nutrients is recommended, in addition to dietary treatment with adequate protein and energy intake, for the management of these complications.[6–8]

Branched-chain amino acid granules are used for the improvement of hypoalbuminemia in patients with decompensated liver cirrhosis,[4,9–11] and several studies have demonstrated their efficacy in reducing complications of liver cirrhosis.[4,12–14] Furthermore, a reduction in

Correspondence: Professor Hisataka Moriwaki, Department of Medicine, Gifu University Graduate School of Medicine, 1-1 Yanagido, Gifu 501-1194, Japan. Email: hmori@gifu-u.ac.jp
Received 13 July 2012; revision 26 August 2012; accepted 27 August 2012.

the risk of hepatic cancer is also reported in patients taking BCAA granules.[12,15–17]

On the other hand, the patients' treatment adherence was not so favorable owing to the size of individual doses and unpleasant taste, causing interruption of treatment[13] or reduction of doses.[4] Although serum albumin level has been shown to improve in a dose-dependent manner based on the prescribed BCAA doses,[10] no studies have investigated exactly how treatment adherence may influence the serum albumin level and prognosis of patients with liver cirrhosis.

We conducted the present analysis to evaluate how treatment adherence may affect the serum albumin level and prognosis in a prospective cohort of 5042 patients with liver cirrhosis who had started BCAA treatment at a fixed dose of three sachets/day in a preceding study.[18]

METHODS

Study design and protocol

THIS WAS A multicenter prospective observational study to determine the incidence of adverse events, including hepatocellular carcinoma (HCC) and cirrhosis-related events, under the actual condition of treatment in patients with decompensated liver cirrhosis who were prescribed BCAA granules between June 2003 and December 2006,[18] and were further followed up thereafter.

A total of 5042 patients with decompensated liver cirrhosis, who presented hypoalbuminemia despite adequate dietary intake, were enrolled in this study at 929 medical institutions in Japan. These patients were p.o. administrated BCAA granules containing 952 mg of L-isoleucine, 1904 mg of L-leucine and 1144 mg of L-valine (Livact Granules, Ajinomoto Pharmaceutical, Tokyo, Japan) at 4.15 g/sachet three times a day after meals.

Patient flow is shown in Figure 1. Of the 5042 patients enrolled, the medical records were not available for 222 patients, and 123 patients were lost to follow up after the initial hospital visit. Thus, the remaining 4697 patients constituted the prospective cohort. Patients meeting any of the following criteria were then excluded, and the remaining 2984 patients were subjected to the analysis: (i) a baseline serum albumin level higher than 3.5 g/dL; (ii) a baseline serum total bilirubin level of 3.0 mg/dL or higher; (iii) unknown duration of study observation; (iv) baseline dosage of prescribed BCAA granules other than three sachets/day; or (v) unknown BCAA treatment adherence for 6 months after the start of study observation.

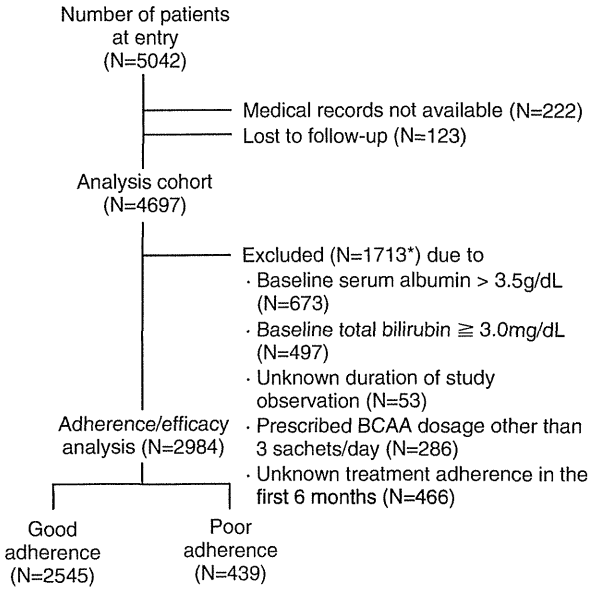

Figure 1 Patient flow. *Among the 1713 patients, 262 were excluded by meeting two or more conditions of the exclusion criteria. BCAA, branched-chain amino acid.

The patients' treatment adherence was evaluated by a questionnaire analysis at the end of the 6-month surveillance period. The questionnaire provided three answer arms who took "nearly all", "approximately half" and "less" of the prescribed dose of BCAA granules at three sachets/day. Each patient was instructed to select one of the above three answer arms that best reflected his/her drug adherence status in the preceding study period.

The primary end-point was the time to onset of the event, defined as hospital admission due to progression of hepatic failure, including ascites, edema, jaundice and hepatic encephalopathy. Changes in liver function during the 6 months were evaluated as the secondary end-point.

This study was conducted in accordance with the Japanese Good Post-Marketing Surveillance Practice.

Statistical analysis

Continuous data were expressed as mean ± standard deviation, and differences in mean values were statistically tested using paired or unpaired Student's *t*-test as appropriate. Categorical variables were compared by Wilcoxon signed rank test, Wilcoxon rank sum test or χ^2-test as required. The cumulative event-free survival rates were estimated using the Kaplan–Meier method

and compared by log–rank test. Any risk factors contributing to the primary end-point were investigated by univariate and multivariate analyses using a Cox proportional hazards model. Data analysis was performed using JMP ver. 9.02 and SAS ver. 9.2 (both SAS Institute, Cary, NC, USA). The level of significance was assessed as two-sided $P < 0.05$.

RESULTS

Patients' characteristics and flow

OF THE PROSPECTIVE cohort consisting of 4697 patients, 1713 were excluded by meeting the exclusion criteria (Fig. 1). Among them, 673 patients had a baseline serum albumin level higher than 3.5 g/dL, 497 patients had a baseline serum total bilirubin level of 3.0 mg/dL or higher, 53 patients had an unknown duration of study observation, 286 patients were prescribed BCAA granules of a dosage other than three sachets/day, and 466 patients reported unknown treatment adherence during the 6 months of study observation. Two hundred and sixty-two patients were excluded by fulfilling two or more conditions of the exclusion criteria. Thus, the remaining 2984 patients were subjected to the adherence/efficacy analysis (Fig. 1). Clinical characteristics of these patients are shown in Table 1. The observation period ranged 6.0–47.9 months, with a median of 21.6 months.

Risk factors for the primary end-point

For the primary end-point, univariate and multivariate analyses using a Cox proportional hazards model identified the following independent factors to influence the development of the event: age, treatment adherence for the 6 months of study observation, previous hepatic cancer, current clinical manifestations, previous clinical manifestations, baseline serum albumin level, platelet count and serum total bilirubin level (Table 2).

Treatment adherence and plasma BCAA/tyrosine ratio

All these variables except treatment adherence have already been documented as risk factors in patients with liver cirrhosis.[19,20] Taking notice of treatment adherence, therefore, 2545 patients who reported to have taken "nearly all" the prescribed doses during the 6-month period comprised the good adherence group and 439 patients who reported to have taken "approximately half" or "less" of the prescribed doses during that period comprised the poor adherence group for further analysis.

Table 1 Clinical characteristics of patients

Characteristics		$n = 2984$
Sex	Male	1584 (53.1%)
	Female	1400 (46.9%)
Age (years)	20–29	1 (0.0%)
	30–39	24 (0.8%)
	40–49	165 (5.5%)
	50–59	530 (17.8%)
	60–69	1038 (34.8%)
	70–79	1024 (34.3%)
	80–89	195 (6.5%)
	>90	7 (0.2%)
	Mean ± SD	66.1 ± 10.1
Cause of liver cirrhosis	HBV	217 (7.3%)
	HCV	1755 (58.8%)
	Alcohol	487 (16.3%)
	PBC	74 (2.5%)
	AIH	63 (2.1%)
	HBV + HCV	16 (0.5%)
	HBV + alcohol	29 (1.0%)
	HCV + alcohol	92 (3.1%)
	HBV + HCV + alcohol	2 (0.1%)
	Other	57 (1.9%)
	Unknown	192 (6.4%)
Treatment adherence (during 6 months)	All	2545 (85.3%)
	Half or less	439 (14.7%)
Previous hepatic cancer	Yes	504 (16.9%)
	No	2454 (82.2%)
	Unknown	26 (0.9%)
Current clinical manifestations	Yes	1568 (52.6%)
	No	1410 (47.3%)
	Unknown	6 (0.2%)
Previous clinical manifestations	Yes	1291 (43.3%)
	No	1670 (56.0%)
	Unknown	23 (0.8%)
Diabetes	Yes	536 (18.0%)
	No	2448 (82.0%)
Serum albumin (g/dL)		3.04 ± 0.36
Platelet (×10 000/μL)		9.73 ± 6.15
AST (IU/L)		67.1 ± 62.8
ALT (IU/L)		47.8 ± 40.9
Serum total bilirubin (mg/dL)		1.30 ± 0.62
BTR		2.95 ± 1.37

For categorical variables, the number of patients and percentage are shown. For continuous variables, the mean ± SD is presented. AIH, autoimmune hepatitis; ALT, alanine aminotransferase; AST, aspartate aminotransferase; BTR, branched-chain amino acid/tyrosine ratio; HBV, hepatitis B virus; HCV, hepatitis C virus; PBC, primary biliary cirrhosis; SD, standard deviation.